

Iris Segmentation and Recognition Algorithms: A Survey

R. P. Ram Kumar

Professor, Department of Computer Science and Engineering,
Malla Reddy Engineering College (Autonomous), Secunderabad, Telangana State, India.

Abstract: The goal of iris recognition is to recognize human identity through the textural characteristics of one's iris muscular patterns. Even though eye color is dependent on heredity, in contrast to this, the iris is independent and uncorrelated even for twins. Out of various biometrics, iris recognition has been acknowledged as one of the most accurate biometric modalities because of its high recognition rate. In this paper, we have studied various well-known algorithms for iris recognition. The result shows that the Daugman's Algorithm gave the highest accuracy of 99.9%.

IndexTerms - Biometrics, Iris Recognition, IrisCode, Iris texture, Similarity measure.

I. INTRODUCTION

In the current technological era, the security plays a vital role. To provide the secured access, the proper authentication becomes mandatory. There are three types of authentication mechanisms, namely, password (something you know), cards/token (something you have) and biometric (something you are). Simple passwords are easy to crack, and harder ones are hard to remember. Even though the cards and tokens are easy to handle, the authentication of the corresponding owner becomes overhead. On the other hand, the biometrics provides both the authentication and identification. If the biometrics is merged with any mechanisms (passwords, cards, and token), then it acts as a two-factor authentication system for security reasons.

Biometric identification utilizes two characteristic features, namely, physiological and behavioral features for individual identification. Physiological characteristic features include face recognition, iris pattern, retinal pattern, ear structure, fingerprint and palm print, whereas the behavioral features include voice pattern, signature, and keystroke dynamics. During the enrollment phase, the biometric features are captured and stored in the database. In the verification phase, the feature of the input image is compared with the features of the stored images. Figure 1 demonstrates the two processes, namely enrollment, and verification, of the biometric authentication system.

During the enrolment phase, an image is acquired, and the template is created and stored in a database or a smart card [Davida et al. (1998)]. During the verification or authentication phase, the presented biometric sample is validated with the already stored template. When the similarity measures are less than the predefined threshold value, then the user is an authenticated user else treated as an unauthorized user. According to [Ratha et al. (2001)], a user may be forging the biometric authentication by compromising the concern biometric identifier only. The other possibility of misuse may occur during the storage of data [Jain et al. (2007)].

1.1 Basics of Iris Recognition Methodologies

Performance of biometric identification is determined by two kinds namely, within-subject and between-subject variability. Characteristics of a person may be categorized as genotypic and phenotypic features. Persons with genetic penetrance shares all their genotypic features such as gender, blood group, DNA sequence, etc., whereas the phenotypic characteristics refer to the actual expression of a feature through the interaction of genotype, development, and environment, such as fingerprint, iris patterns, etc., which is termed as biometric recognition. Among the variety of biometric features like iris, retina, face, ear, voice, hand geometry, veins, DNA, gait, and fingerprint, the role played by iris recognition is amicable. Various studies show that the iris is so unique that no two irises are alike, even among identical twins, in the entire population. Further, it was explored that there were more than 400 distinguishing characteristic features, also called as Degrees of Freedom (DOM), that are used to identify an individual. Some of the identifiable characteristics are contraction, furrows, striations, pits, collagenous fibers, filaments, crypts, serpentine vasculature, rings, and freckles [Wildes (1997)].

The iris is an internal organ and also stable throughout the entire lifespan. Due to these unique features, iris recognition is considered as accurate, reliable, and against artifice, when compared with other biometric recognition methods. Given this, the statistical probability that two irises would be the same is estimated at 1 in 10^{72} [Daugman (1993)].

In practice, the iris pattern must be extracted from the image before analysis. The pattern of an iris, once captured by an infrared camera, can be analyzed, and the resulting features can be used to quantitatively and positively distinguish one eye from another. Commercial systems today utilize the patented Daugman's algorithm [Daugman (2002)], to detect the iris pattern using circular edge detection. They are unable to successfully locate the iris pattern to proceed to recognition and matching. However, most of the

existing algorithms claimed that the iris region is circular in nature. The process for biometric recognition using the iris can be described as a series of steps that make up an architectural framework. This framework for recognition can be divided into subcomponents as shown in Figure 1, based on [Etter (2005)], each with its own set of algorithms governing the tasks required of it.

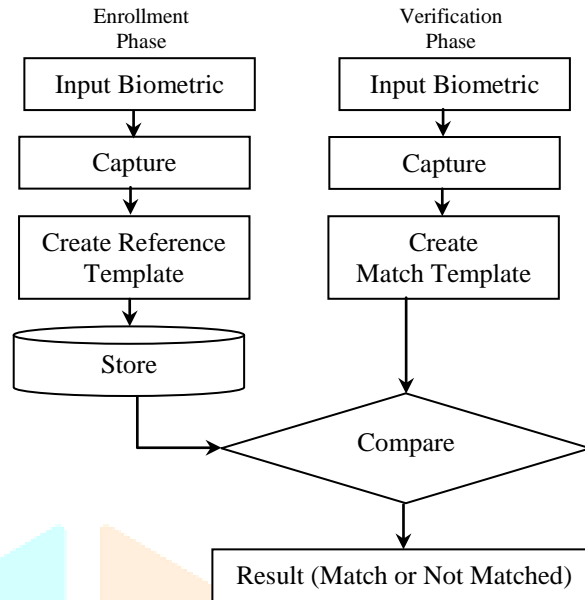


Figure 1 Processes involved in Biometric Recognition

These subcomponents are:

- **Image Preprocessing:** The first step is to determine the location of the pupil. Then, image adjustments are made for illumination, scale and rotation variations.
- **Iris Detection:** This stage involves locating the outer edge of the iris and separating it from the remaining portions of the eye. The data representing the iris is called the iris pattern.
- **Iris Code Generation:** Here, templates (sometimes referred to as the IrisCode) for authorized individuals are created and stored in the database.
- **Comparison:** This stage performs identification/verification by comparing the new test code of the presented iris to the IrisCode that have been stored in a database. This stage computes the differences between the test iris code and the stored templates.
- **Decision:** At the final stage in the iris identification process, a decision is made based on comparisons performed in the preceding stage. Typically, a system will return either a match or no match.

II. COMPARISON OF IRIS RECOGNITION ALGORITHMS

2.1 Daugman's Approach

In iris localization, the separation of inner and outer boundaries of the iris and the exclusion of eyelids (if they intrude) are done. Integrodifferential operator represented in Equation 1 accomplishes these detections,

$$\max_{(r, x_0, y_0)} \left| G_{\sigma}(r) * \frac{\partial}{\partial r} \oint_{r, x_0, y_0} \frac{I(x, y)}{2\pi r} ds \right| \quad (1)$$

where, contour integration is parameterized for size and location coordinated r, x_0, y_0 at a scale of analysis set by $G_{\sigma}(r)$ is performed over image data $I(x, y)$.

Then, a double-dimensionless coordinate system is defined which is invariant to changes in pupillary construction and size. The detailed iris pattern is encoded into a 256-byte IrisCode by demodulating it with 2D Gabor wavelets [Daugman (1980), Daugman (1988), Daugman (1995)]. The computed IrisCode for any eye is invariant under translations, and dilations (size changes), including changes in the pupil relative to the iris diameter. However, the phasor information scrolls in phase as the iris are rotated, due to the tilt of the head or camera or due to torsional rotation of the eye in its socket. In this method, decisions about personal identity were done with very high confidence, even though if the 30% of the bits being wrong, due to the poor quality of resolution, focus, occlusions due to eyelashes and eyelids, contact lenses, specular reflections from cornea or eyeglasses, and noise. The deciding factor for identifying the individual was done by the Hamming Distance (HD) distributions of the iris patterns. The histogram in figure 3 compares 222,743 pairs of unrelated IrisCode, by vector Exclusive-OR operation.

The data observed are standard deviation (SD)=0.0306, mean=0.498 and Degrees of Freedom (DoF)=266. The experimentation on identical genetic irises (324 pairs) concluded that the iris recognition does not depend on genotypic and is a purely phenotypic feature. The data observed were SD=0.03108, mean=0.497 and DOF=259. This indicates that the phase structure extracted from irises by phasor demodulation process is purely phenotypic and not genotypic.

At the crossover point 0.342, the fractions of disagreeing bits for false acceptance error and false rejection errors are equal to 1 to 1.2 million for the fitted pair of distributions. With this confidence levels against a false match, one can afford to search even a planetary size database.

2.2 William's Approach

After the iris image acquisition, the suitable area for feature extraction and analysis is to be identified. By using an exclusive algorithm [Williams (2001)], the areas covering the iris regions are excluded, and the boundaries of pupil and iris are identified, through the field optimization process. Then the features of iris are analyzed and digitized into a 512 byte (4096 bit) IrisCode of two equal parts. The first half represents the features and the second half for comparison. The Hamming Distance (HD) is used as a measure for matching the IrisCode and is calculated as the ratio between non-matched and matched bits. At HD 0.342, the probability of a false reject is approximately the same as the probability of a false accept, i.e., while comparing the presented and referenced IrisCode record, if they differ by 34.2% & or more, they are considered to have emanated from different irises. All these processes need 2 to 3 seconds range even with the very large databases.

2.3 Zhu's Approach

In this approach [Zhu et al. (2000)], the algorithm provides translation, rotation, and scale invariant through texture analysis using Gabor filtering and wavelet transform. For preprocessing, the iris boundaries were considered as circles and are not concentric. The pupillary and limbic boundaries are detected by thresholding operation and maximizing the perimeter changes in the normalized sum of gray values. Later, the normalization is carried out to form the uniform dimension. By using local histogram equalization, the iris image is enhanced for feature extraction.

The analysis of iris uses multi-channel Gabor filter, and wavelet transforms. The multi-channel Gabor filtering technique is inspired by the processing of pictorial information in the human visual cortex involving a set of parallel and cortical channels which are treated as bandpass filters [Tan (1992)]. Each cortical channels are considered as pair of Gabor filters and is given by Equation (2).

$$\begin{aligned} h_x(x, y) &= g(x, y) \cdot \cos[2\pi f(x \cos\theta + y \sin\theta)] \\ h_y(x, y) &= g(x, y) \cdot \sin[2\pi f(x \cos\theta + y \sin\theta)] \end{aligned} \quad (2)$$

Where, $g(x, y)$ is a Gaussian function, ' f ' is the central frequency with the ranges 2, 4, 8, 16, 32 & 64 cycles/degree and ' θ ' is the orientation for filtering at 0° , 45° , 90° , and 135° respectively. This leads to fetch the iris features extraction at 24 output images (with six central frequencies and four degrees). The wavelet transform is applied to have better texture discrimination [Laine (1993)]. This results in sub-images at various resolution levels. Now the features (variance and mean) from each sub-image are extracted. Weighted Euclidean Distance (WED) is used for matching process and calculated using the Equation (3).

$$WED(k) = \sum_{i=1}^N \frac{(f_i - f_i^{(k)})^2}{(\delta_i^{(k)})^2} \quad (3)$$

Where f_i is an i th feature of unknown iris, $f_i(k)$ is the i th feature of iris k , $\delta_i(k)$ is the standard deviation of iris k , and N is the total number of features extracted from a single iris. A classification rate of 93.8% was obtained when applying Gabor filtering technique and Wavelet transform under WED. Even though this algorithm extracts global texture features, it uses only a few selected regulations or scales for the matching process.

2.4 Poursaberi's Approach

In the preprocessing phase, the captured iris image is converted into a grayscale image of size 256 x 256 [Poursaberi (2005b)]. To eliminate the artifacts and reflections due to light on eye image, the following steps are adopted; (a) Compute the complement of the image, (b) Fill the holes in the intensity image, and (c) Compute the complement of the image again to get the original grayscale image. Now, the resulting image is free from reflections in the pupil region. The pupil's inner edge is detected using thresholding method. The image obtained is filtered with Extended Minima (EM) morphology operator to suppress the entire intensity image below a certain scalar value. By choosing an appropriate scalar in EM transform, the outer boundary of the iris is detected perfectly.

After locating the iris boundaries iris, the circle and radius of two circles are determined in a fast and simple manner [Poursaberi (2004)]. The modified Daugman's RSM is used for normalization process. Histogram Equalization (HE) and Daubechies2 wavelet are applied for image enhancement and feature extraction process, respectively. The resulting will be four-level wavelet decomposition contents and approximation coefficients of unwrapped iris image of size 512 x 56 pixels; after four times decomposition, the size of last part is 6 x 34. Therefore, an iris image is represented as binary feature vector depending on the sign of each coefficient. Then the matching process is based on Euclidean Distance (ED) and determined by Equation (4).

$$ED = \frac{1}{N} \left(\sqrt{\sum_{i=1}^N (\text{CodeA}(i) - \text{CodeB}(i))^2} \right) \quad (4)$$

where N is 408, CodeA is input image's feature vector, and CodeB is database image.

The minimum ED shows that the iris belongs to the same class (accept) and the maximum value shows the different class (reject). When evaluated with 252 images from CUHK dataset, the recognition rate was found to be 95.71%. Under the reasonable range, the factors such as noise, illumination, contrast, and rotation will not influence the efficiency of this method [Poursaberi (2005a)].

2.5 Subbarayudu's Approach

Here [Subbarayudu (2008)], a modified approach is used for iris localization and normalization methods. For iris localization, the following steps are adopted: (1) Conversion into grayscale, (2) Identification of holes, (3) Canny operator based edge detection [Canny (1986)], (4) Identification of pupil course center by choosing the threshold value using gray level histogram [Otsu (1979)], and (5) Identification of iris boundaries using circular Hough transform.

When compared with [Wildes (1997)] and [Ma (2004)], the proposed method has less computational cost. The normalized strip is enhanced using a low-pass Gaussian filter. HD is used for the matching process. When evaluated with 2000 images from CASIA database, resulted in 95% recognition rate and found to be higher than the method represented in [Ma (2004)].

2.6 Basit's Approach [24]

In this approach [Basit et al. (2005)], the input image is converted into gray scale image. The exact pupil center is determined to form the rough estimation of pupil center. Then the pupil radius is determined using the average of distance values from among the pupil center and limbic boundary. The resultant image is convolved with a 2D Gaussian operator to detect the limbic boundary [Huang et al. (2002)], with center at (x_0, y_0) and is given by the Equation (5).

$$G(x, y) = \frac{1}{2\pi\sigma^2} e^{-\frac{(x-x_0)^2+(y-y_0)^2}{2\sigma^2}} \quad (5)$$

where, ' σ ' is standard deviation, that smoothes the image. After this, canny operators with threshold values 0.005 and 0.1 as lower and upper limits are applied to find the boundaries of iris. The iris radius determination process is identical to pupil radius identification process. For normalization process, the hollow iris disk is mapped into rectangular region by using Equation (6).

$$I(x(r, \theta), y(r, \theta)) \rightarrow I(r, \theta) \quad (6)$$

where, ' r ' lies between $[0, 1]$ and ' θ ' is the circular angle between $(\theta, 2\pi)$. As unwrapping of iris starts from inner and proceeds towards the outer boundary, ' m ' concentric circles are obtained and then ' n ' samples are collected on each concentric circles so that $m \times n$ matrix will be the resulting rectangular iris band. Then it is treated with histogram equalization for enhancement. For each class, four irises are trained and mean of the trained irises are subtracted from each iris and is determined by Equation (7).

$$M_{i \times j} = \frac{1}{k} \sum_{p=1}^k I_p \quad (7)$$

where, ' k ' is a total number of irises, and ' I_i ' is the i th iris image. Eigenvectors are calculated for each iris, and highest Eigenvalue is treated as a distinct feature of that iris. Euclidean distance is used for the matching process and if it is minimum, accept as match else rejects as an imposter. When evaluated with 140 images, the recognition rate was found to be 94.28%. The failure rate may be diminished with more training images. Main drawbacks of this system are, (a) the system needs retraining when the new classes were added, and (b) the more the class, the increase in computation time.

2.7 Birgale's Approach

The main motivation of this approach [Birgale (2010)] is to reduce the computational time thereby avoiding the normalization step and is summarized as follows: (1) a mask is specially designed to avoid occlusions due to eyelid and eyelash, (2) Iris signature size is very much reduced, and (3) Resulted in reduced processing time and improvement in recognition time.

For segmentation process, a mask is specially designed, so that it eliminates the occlusions due to eyelid and eyelashes. After this process, Discrete Wavelet Transform (DWT) is used for feature extraction and is represented by Equation (8).

$$DWT = \sum_{k=1}^{\infty} \sum_{l=-\infty}^{+\infty} q(k, l) \psi(2^{-k}t - l) \quad (8)$$

The advantage of Wavelet analysis lies in the variable size window region, and it is a time-frequency region, rather a time scale. To get the analysis results accurate and efficient, the scales and positions are selected based on the powers of two so-called dyadic scales and positions. This method gave better performance regarding FAR, FRR, speed and efficiency with 1×24 size signatures. With the designed masks, each eye image is filtered with it. For every filtered image, three-level Wavelet decompositions are obtained. Comparisons with different mask shapes (such as a circle, hexagon) are carried out to check the efficiency of the proposed method. The Iris signatures are calculated using Standard Deviation and First level energy, given by Equation (9).

$$\text{Energy} = \sum_0^{M-1} \sum_0^{N-1} |X(m, n)| \quad (9)$$

where, $X(m, n)$ is a discrete function, whose energy is to be calculated. SD is given by Equation (10).

$$\sigma_k = \frac{1}{M \times N} \sum_{i=1}^M \sum_{j=1}^N E[W_k(i, j) - \mu_k] \quad (10)$$

where, $W(i, j)$ is the k th wavelet decomposed sub-band, $M \times N$ is wavelet decomposed sub-band, and μ_k is mean value of k th decomposed sub-band. Here standard wavelets are used to extract Iris textures, with three level decompositions. Obtained results are compared with previous methods [Daugman (1993), Zhu et al. (2000), Poursaberi (2005b), Subbarayudu (2008), Basit et al. (2005), Birgale (2010)]. Observation shows that mask optimization removes eyelid and eyelash occlusions with improved efficiency. For matching process, ED is used and is given by Equation (11).

$$D_{(x,y)}^{\text{Eucl}} = \sqrt{\sum_{i=0}^N (x_i - y_i)^2} \quad (11)$$

So far obtained results are compared with various existing methods, such as with normalization, without normalization, with Daubchies wavelets, and with Haar wavelets. This method's efficiency was found to be 99.48% with CASIA database version 2003 [CASIA-IrisV3]. Moreover, while comparing the processing speed with normalization and without normalization, which yields the time economy of 0.3342 seconds with this method (without normalization). Though Daugman's method gives the accuracy of 99.90% with the Iris Signature of length 1 x 2048 size, this method gives the accuracy of 99.474% with a very small size 1 x 24 of IrisCode and also provides an improvement in the processing speed.

III. CONCLUSION

This paper presents a review of the existing algorithms available for iris recognition. Iris recognition technology can provide more accurate results for human identification. The algorithms are divided into four steps namely, localization, normalization, feature extraction and matching. Among the experimental results of several algorithms, Daugman's algorithm gives maximum accuracy (99.9%). Thorough study is under process on various Iris recognition algorithms regarding diminishing the processing time without affecting the recognition accuracy.

REFERENCES

- [1] Argles, D. *et al.* (2007): An Improved Approach to Secure Authentication and Signing, Advanced Information Networking and Applications Workshops, AINAW '07.
- [2] Basit. A. *et al.* (2005): Efficient Iris Recognition Method for Human Identification, Proceedings of World Academy of Science, Engineering and Technology, Volume 4, ISSN 1307-6884, pp. 24-26.
- [3] Birgale Lenina. and Kokare. M. (2010): Iris Recognition Without Iris Normalization, Proceedings of Journal of Computer Science 6 (9), ISSN 1549-3636, pp. 1042-1047.
- [4] Bolle, R. *et al.* (2004). Guide to Biometrics, New York, Springer Professional Computing.
- [5] CASIA-IrisV3, <http://www.cbsr.ia.ac.cn/IrisDatabase.htm>
- [6] Canny. J. (1986): A computational approach to edge detection, IEEE Transaction Pattern Analysis and Machine Intelligence, 8 (6), pp. 679-698.
- [7] Daugman. J. G. (1980): Two-dimensional spectral analysis of cortical receptive field profiles, Vision Research, Vol. 20, No. 10, pp. 847-856.
- [8] Daugman. J. G. (1988): Complete discrete 2D Gabor transforms by neural networks for image analysis and compression, IEEE Trans. Acoustics, Speech, and Signal Processing, Vol. 36, No. 7, pp. 1169-1179.
- [9] Daugman. J. G. (1993): High Confidence Visual Recognition of Persons by a Test of Statistical Independence, IEEE Transactions on Pattern Analysis and Machine Intelligence, Vol. 15, No. 11, November, pp. 1148-1161
- [10] Daugman. J. G. and Downing. C. J. (1995): Demodulation, predictive coding, and spatial vision, Journal of the Optical Society of America A, 12(4), pp. 641-660.
- [11] Daugman. J. G. (2002): How iris recognition works, Proceedings of International Conference on Image Processing, Vol. 1, pp. 33-36
- [12] Davida, G. I. *et al.* (1998): On enabling secure applications through off-line biometric identification, Proceedings IEEE Symposium on Security and Privacy, Oakland California U.S.A, IEEE Computer Society.
- [13] Etter. Delores M. and Bonney. L. Ens Bradford. (2005), Professor, Electrical Engineering Department, United States Naval Academy, and United States Navy, Small Business Technologies, June 29.
- [14] Huang. Y. P. *et al.* (2002): An efficient iris recognition system, Proceedings of first International Conference Machine Learning and Cybernetics, Beijing, 4-5, November.
- [15] Jain, A. K. *et al.* (2007): Biometric Template Security, EURASIP Journal on Advances in Signal Processing, Hindawi Publishing Corporation.
- [16] Laine. A. and Fan. J. (1993): Texture Classification by Wavelet Packet Signatures, IEEE Transaction Pattern Analysis Machine Intelligence., vol.15, pp.1186-1191.
- [17] Ma.Li, *et al.* (2004): Efficient Iris Recognition by Characterizing Key Local Variations, IEEE Transactions on Image processing, Vol. 13, pp. 739-750, June.
- [18] Otsu. N.(1979): A threshold selection method from gray level histograms, IEEE Trans System, Man and Cybernetics, SMC-9, pp. 62-66.
- [19] Poursaberi. A. and Araabi. B. N. (2004): A Fast Morphological Algorithm for Iris Detection in Eye Images, 6th International Conference on Intelligent Systems, Kerman, Iran.
- [20] Poursaberi. A. and Araabi. B. N. (2005a): A Binary Representation of Iris Patterns for Individual Identification: Sensitivity Analysis, PRIP'05, Eighth International Conference on Pattern Recognition and Information Processing May 18-20, Minsk, Belarus,
- [21] Poursaberi A. and Araabi. B. N. (2005b): A Novel Iris Recognition System Using Morphological Edge Detector and Wavelet Phase Features, ICGST-GVIP Journal, Volume (5), Issue (6), pp. 9-15, June.
- [22] Ratha, N. K. *et al.* (2001): Enhancing security and privacy in biometrics-based authentication systems, IBM systems Journal 40(3), pp. 614-634.
- [23] Subbarayudu.V. C. and Prasad. Munaga V. N. K. (2008): A Novel Iris Recognition System, Third International IEEE Conference on Signal-Image Technologies and Internet-Based System, pp. 883-887.
- [24] Tan. T. (1992): Texture Feature Extraction Via Visual Cortical Channel Modelling, Proc. 11th IAPR International Conference. Pattern Recognition, Vol. III, pp.607-610.

- [25] Wildes. R. (1997): Iris Recognition: An emerging biometric technology, Proceedings of the IEEE, vol.85, no.9, September, pp. 1348-1363
- [26] Williams. Gerald O. (2001): Iris Recognition Technology, Iridian Technologies, Inc.
- [27] Zhu. Yong. *et al.* (2000): Biometric Personal Identification Based on Iris Patterns, National Laboratory of Pattern Recognition (NLPR), Institute of Automation, Chinese Academy of Sciences, China.

